Hindawi Publishing Corporation
Mathematical Problems in Engineering
Volume 2015, Article ID 502372, 11 pages
http://dx.doi.org/10.1155/2015/502372

*Research Article*

# Fault Characteristics and Control Strategies of Multiterminal High Voltage Direct Current Transmission Based on Modular Multilevel Converter

**Fei Chang,[1] Zhongping Yang,[1] Yi Wang,[2] Fei Lin,[1] and Shihui Liu[1]**

[1]*School of Electrical Engineering, Beijing Jiaotong University, Beijing 100044, China*
[2]*School of Electrical Engineering, Tsinghua University, Beijing 100084, China*

Correspondence should be addressed to Fei Chang; 14117397@bjtu.edu.cn

Received 22 April 2015; Revised 26 May 2015; Accepted 27 May 2015

Academic Editor: Xiaosong Hu



The modular multilevel converter (MMC) is an emerging voltage source converter topology suitable for multiterminal high voltage direct current transmission based on modular multilevel converter (MMC-MTDC). This paper presents fault characteristics of MMC-MTDC including submodule fault, DC line fault, and fault ride-through of wind farm integration. Meanwhile, the corresponding protection strategies are proposed. The correctness and effectiveness of the control strategies are verified by establishing a three-terminal MMC-MTDC system under the PSCAD/EMTDC electromagnetic transient simulation environment.

## 1. Introduction

The rapid development of power electronic technology has promoted the development of sustainable transportation and power systems [1–5]. The modular multilevel converter (MMC) was first introduced in 2001 [6] and has drawn great attention due to its excellent output waveform and high efficiency [7, 8]. As a new topology of voltage sourced converter based high voltage direct current transmission (VSC-HVDC), MMC-HVDC has prodigious potential in transmission and distribution applications, such as wind farm connection [9–13], multiterminal operation [14], and a passive network power supply [15].

Multiterminal HVDC transmission based on MMC (MMC-MTDC) is defined as the flexible HVDC transmission system which has three or more voltage source converters (VSCs) under the same DC grid [16]. Its prominent feature lies in providing multiple power supplies, power receiving in multiple places. As a more flexible and efficient power transmission mode, MMC-MTDC shows great potential in renewable energy connection, urban DC distribution network, and so on. In the world, there are only two MMC-MTDC projects and they are all in China [17]. One of which is Nanao three-terminal MMC-MTDC project constructed in Dec. 2013 which is the world's first MMC-MTDC project; the other one is Zhoushan five-terminal MMC-MTDC project constructed in Jul. 2014 which is the world's largest number of terminals in MMC-MTDC projects.

At present, the research of MMC-MTDC is focused on DC voltage stability [17], which can be divided into two categories, including control with communication or no communication. The control with no communication is basically adopted in the actual project which includes DC voltage slope control and DC voltage deviation control. However, the related research on fault protection is also rarely reported [18], in which, a multipoint DC voltage control strategy based on DC voltage margin method is proposed. Furthermore, the impact of different DC faults of the system is analyzed and the corresponding control and protection strategies are given. This paper has been further research on fault characteristics and control strategies of MMC-MTDC, including submodule fault, DC line fault, and fault ride-through of wind farm integration.

## 2. MMC-MTDC System

MMC-MTDC system is composed of three or more MMC converter stations and DC power transmission interconnection lines, as shown in Figure 1. Wherein, the structure of

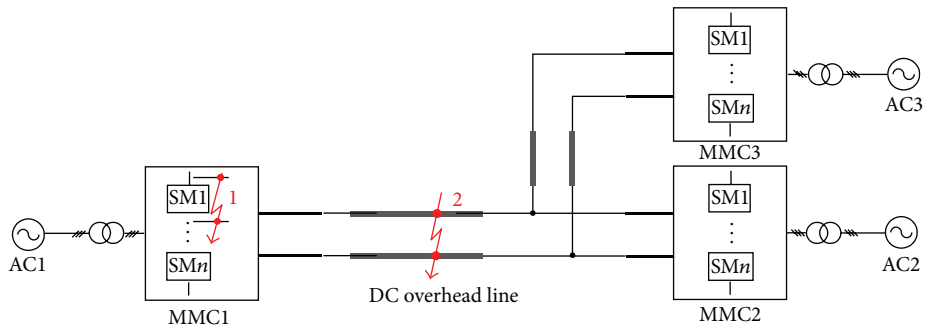


Figure 1: Structure of MMC-MTDC system.

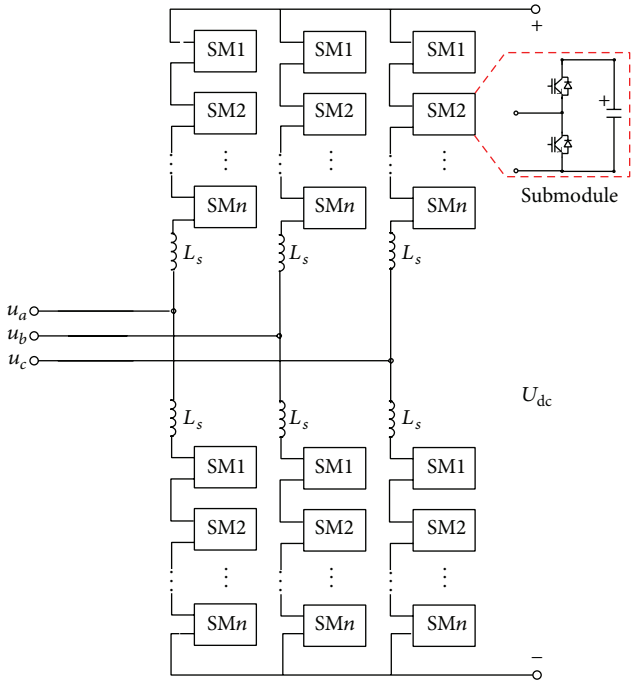


Figure 2: Structure of MMC converter station.

MMC converter station is shown in Figure 2. The system has the advantages of providing multiple power supplies, power receiving in multiple places, and linking several AC systems or separating one AC system into several independent grids.

*2.1. Topology of MMC.* The main circuit topology of a three-phase MMC is shown in Figure 2; the basic circuit unit of MMC is known as submodule (SM). Each bridge arm is constructed by a certain number of submodules and an arm reactance $L$ in series. The MMC topology can change the output voltage and power level of converter in a flexible way, only by changing the number of submodules. As a consequence, the MMC topology has less switching losses and harmonic distortion. In addition, the MMC topology has positive and negative DC bus, which is especially suitable for HVDC applications.

*2.2. Mathematical Model of MMC.* Considering the circumstances of bridge reactance, the simplified equivalent circuit of MMC is illustrated in (1), where $u_{sa}$, $u_{sb}$, and $u_{sc}$ are the fundamental components of the three-phase voltage in AC side, respectively. $i_{sa}$, $i_{sb}$, and $i_{sc}$ are the fundamental components of the three-phase current in AC side, separately. $L$ is the sum of bridges' inductance which is in single-phase as well as leakage inductance of the converter transformer. $R$ is the equivalent resistance which consists of bridge reactor and converter transformer. $u_a$, $u_b$, and $u_c$ are the fundamental components of the three-phase voltage in converter side, respectively [19]:

$$\begin{aligned} L\frac{di_{sa}}{dt} + i_{sa}R &= u_{sa} - u_a, \\ L\frac{di_{sb}}{dt} + i_{sb}R &= u_{sb} - u_b, \\ L\frac{di_{sc}}{dt} + i_{sc}R &= u_{sc} - u_c. \end{aligned} \tag{1}$$

## 3. Submodule Fault

Normally, the submodule fault occurs mainly due to overvoltage, overcurrent or excessive $dv/dt$, $di/dt$, or the control fault due to false triggering pulses. The system operation should not be influenced by one or several fault submodules, so the submodule needs fault redundancy protection to make the converter have the ability of fault tolerance and improve the reliability of the system.

*3.1. Fault Characteristics.* Taking phase $a$, for example, the upper and lower arms energy of MMC $W_{pa}$ and $W_{na}$ can be expressed as [20]

$$\begin{aligned} W_{pa} &= \frac{1}{2}CNu_{cpa}^2 \\ &= \int_0^T \frac{U_{dc}}{2}(1 - m\cos\omega t)\, i_{pa}dt + \frac{1}{2}CNU_C^2, \\ W_{na} &= \frac{1}{2}CNu_{cna}^2 \\ &= \int_0^T \frac{U_{dc}}{2}(1 + m\cos\omega t)\, i_{na}dt + \frac{1}{2}CNU_C^2, \end{aligned} \tag{2}$$

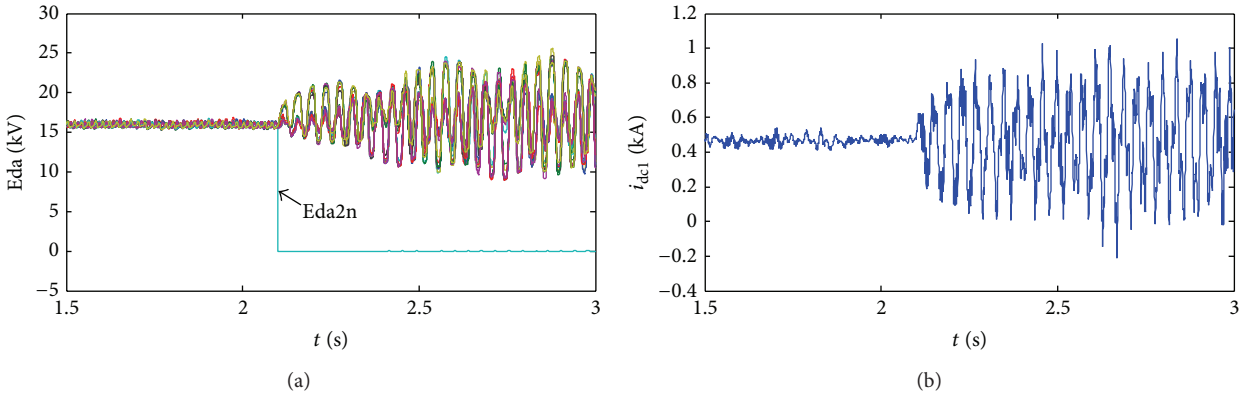


Figure 3: Fault characteristics of submodule. (a) Capacitor voltage of submodules. (b) DC current.

wherein $C$ is capacitance value; $N$ is the number of submodules of each bridge arm; $u_{cpa}$, $u_{cna}$ are, respectively, any submodule voltage of upper and lower arms of phase $a$; $T$ is frequency cycle; $U_{dc}$ is DC voltage; $m$ is voltage modulation ratio, which ranges within $(0, 1]$; $i_{pa}$, $i_{na}$ are, respectively, the upper and lower arms' currents of phase $a$; and $U_C$ is the rated voltage of submodule during normal operation.

By formula (2), it can be seen, when the submodule of upper bridge arm of phase $a$ was fault and bypass, the number of submodules of bridge arm will be less than $N$. In this case, the energy of upper bridge arm of phase $a$ will be less than the other bridge arm, causing the fluctuation of submodule capacitor voltage increase, eventually leading to fluctuations in DC current.

This part describes short-circuit fault of submodule caused by false triggering pulses which correspond to a fault at point 1 in Figure 1 and its simulation parameters are shown in Table 1. Moreover, the simulation waveforms of fault characteristics of submodule are shown in Figure 3. When $t = 2.1$ s, fault occurs in number 2 submodule of lower bridge arm of MMC1 phase $a$ because the upper and lower IGBT simultaneously turned on. Figure 3 shows that the capacitor voltage of fault submodule rapidly drops to 0 that means this submodule stops working and the output voltage of the fault phase will decrease. In addition, because of the parallel connection of three phases, DC current oscillates between the fault phase and the other two phases and may flow into bridge arm and pass through IGBT to cause the fluctuation of capacitor voltage of submodule.

*3.2. Fault Redundancy Protection.* Redundancy protection in cascaded H-bridge converter obtains lots of research and can be classified into two methods [21, 22].

*Method One.* In normal working state, the minority of redundancy submodules are in hot standby mode and the majority are in cold standby mode. Once the submodule fails, the hot standby submodules will replace the cold standby ones and the cold standby submodules will become hot state. The shortcoming is that it takes some time for the action of redundancy submodules and capacitor recharging.

Table 1: Simulation parameters of MMC-MTDC system.

| Parameters | Values |
|---|---|
| Rated capacity of MMC1 | 100 MVA |
| Rated capacity of MMC2 | 50 MVA |
| Rated capacity of MMC3 | 25 MVA |
| Transformer ratio of MMC1 ($Y/\Delta$) | 110 kV/86 kV |
| Transformer ratio of MMC2 ($Y/\Delta$) | 110 kV/86 kV |
| Transformer ratio of MMC3 ($Y/\Delta$) | 110 kV/86 kV |
| DC voltage | 160 kV |
| Number of submodules of bridge arm | 10 |
| Modulation strategy | Nearest level modulation |
| Capacitor voltage balancing strategy | Capacitor voltage sort |
| Control mode of MMC1 | $U_{dc}, Q$ |
| Control mode of MMC2 | $P, Q$ |
| Control mode of MMC3 | $P, Q$ |

*Method Two.* The redundant submodules will not be in hot standby state or in cold standby state but will be directly involved in the normal operation. And once fault occurs in the submodules which are being bypassed, DC voltage will be shared by the remaining submodules in the bridge arm. In order to maintain symmetric operation, the remaining normal operation phases can be bypassed by the same number of submodules in fault phase.

By analyzing the redundancy protection method of cascaded H-bridge converter, this paper proposes a redundancy protection method of MMC. This method will bypass the monitored submodules when fault occurs and then bypass the same number of submodules in the other bridge arm of the same phase to keep the upper and lower bridge arms symmetric. Finally by adjusting the control strategies of MMC a transition is achieved from a full submodules operation mode to $(N - x)$ submodules operation mode, where $X$ means the number of fault submodules. Generally, $x < 4$. If $x \geqslant 4$, the system should stop.

Taking that fault occurring in one submodule, for example, the specific processes of fault redundancy protection are shown in Figure 4.

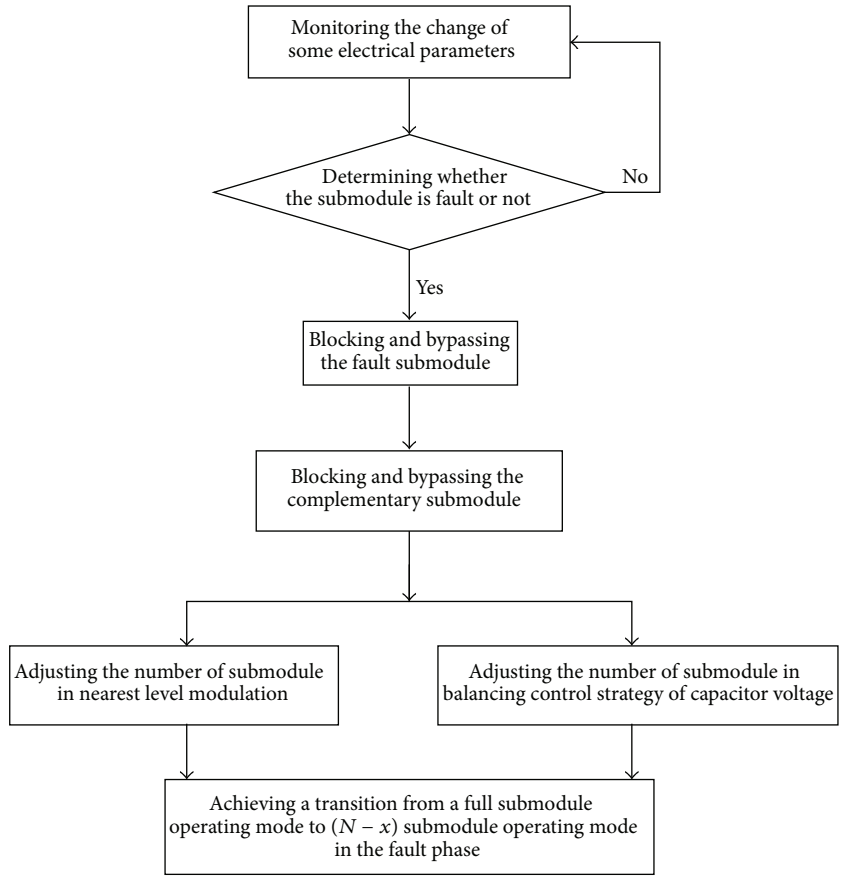


Figure 4: Protection strategies flow chart of submodules fault.

(1) Monitor some electrical parameters including capacitor voltage, capacitor current, and PWM pulses. Once the submodule is at fault, block the fault submodule and bypass it. At this time, the number of submodules in the fault bridge arm changes to $(N - x)$, while the number of submodules in nonfault arm bridge of the same phase is still $N$.

(2) To maintain a constant DC voltage and the same number of submodules in the upper and lower bridge arms of the same phase, it is needed to bypass $x$ submodules in another arm bridge of the same phase. At this time, the total number of submodules in the fault phase becomes $2 * (N - x)$, the number of conduction submodules becomes $(N - x)$, and the capacitor voltage of each submodule rises to $U_{dc}/(N - x)$.

(3) The number of submodules will affect the control strategies of pulses and DC balance; therefore the number of submodules needs to be adjusted correspondingly in the two control strategies. For example, the total number of levels in NLM (Nearest Level Modulation) should be reduced by one, from $(N + 1)$ to $N$; sorting control should only work in the remaining $2 * (N - 1)$ submodules.

But it is important to note that the redundancy protection should cooperate with other protections. After the fault submodule and its complementary submodule being bypassed, because of the three-phase is in parallel, the normal phase will charge the capacitor of the remaining submodules of the fault phase and the capacitor voltage of the fault phase will gradually rise to $U_{dc}/(N - x)$, so the fault phase inevitably undergoes transient process of DC current rising. The transient process may cause the bridge arm short-time overcurrent and the overcurrent will disappear after one cycle. Because the overcurrent time is too short to accumulate enough heating power to burn the device, and the submodule fault should not cause overcurrent protection of the entire bridge arm to act, this lastly causes the whole converter to block or even shut down. Therefore it is reasonable to set bridge arm overcurrent protection threshold and submodules protection threshold or to extend the action time of bridge arm overcurrent protection to prevent the protection malfunction.

The simulation after adding redundancy protection is shown in Figure 5. Because of the rapid blocking of the 2nd fault submodule of lower bridge arm in $a$ phase (Eda2n), Eda2n retains a certain amount of capacitor voltage, the capacitor voltage of the complementary submodule remains near the rating, the capacitor voltage of the rest of the normal submodules in the fault phase rises to rating $N/(N - 1)$ times of rating value and will be stable after a short transient process

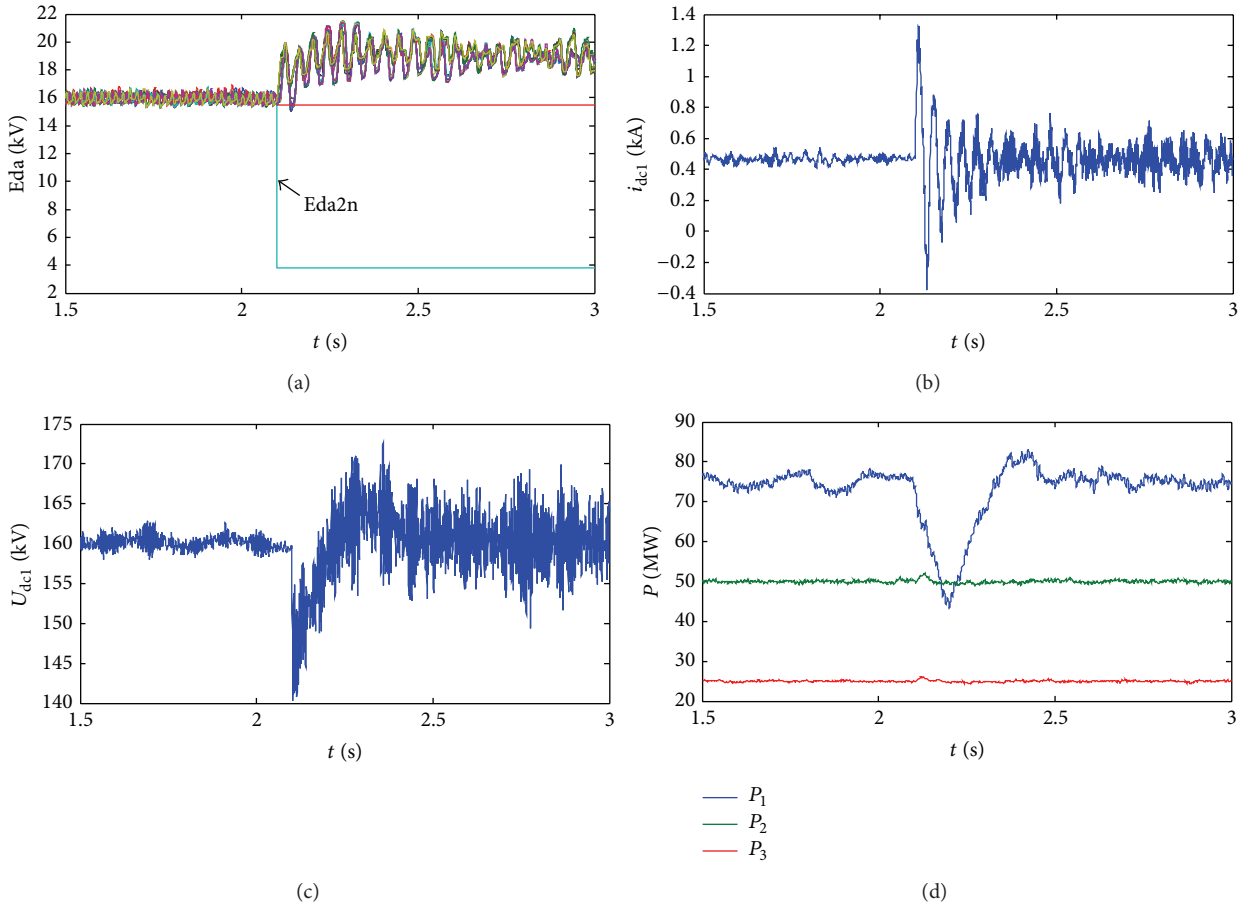


FIGURE 5: Simulation effect after adding fault redundancy protection. (a) Capacitor voltage of submodule of phase *a*. (b) DC current. (c) DC voltage. (d) Active power transmission.

(as shown in Figure 5(a)); the oscillation component of DC current gradually decays to zero (as shown in Figure 5(b)); and DC voltage stability and power transmission normal are shown in Figures 5(c) and 5(d). In summary, the redundancy protection can make the entire system stable when the fault occurs in submodule.

## 4. DC Line Fault

MMC-MTDC is a potential candidate for renewable energy integration over long distances. DC fault is an issue that MMC-MTDC must deal with, especially for the nonpermanent faults when using overhead lines. This section proposed a protection scheme to implement fast fault clearance and automatic recovery for nonpermanent faults on DC lines.

DC overhead line may cause bipolar short-circuit fault due to tree branches. Compared with unipolar ground short-circuit fault, the probability of bipolar short-circuit fault is smaller, but the fault consequences are much more serious. So it is necessary to research fault feature and design fault protection specially.

Most of the overhead line faults are nonpermanent faults and should not result in the system outage, so the system should automatically restart after fault source disappeared and quickly restore power supply. Therefore, the protection is designed with the following objectives. Firstly, IGBT and freewheeling diode should be protected. Secondly, the protection should eliminate DC arc of the fault point under the premise of still working. Thirdly, the system can automatically restart and quickly restore power supply after fault source disappear and DC arc extinguish for nonpermanent fault, but the system needs outage and overhaul for permanent fault. Specific protection methods are as follows.

*4.1. Double Thyristor Switches.* A single thyristor is usually enough if the aim is just to protect the diode from overcurrent. In this paper, in order to make MMC able to quickly clear the fault current and restart power transmission after nonpermanent faults on DC overhead line, double thyristor switches are alternatively employed as shown in Figure 6. The two thyristors are controlled by the same gate signal. During normal operation, the thyristor switches are kept in off-state condition. During DC fault, the thyristor switches are switched on. Since bidirectional thyristor switches are employed, not only is the fault current transferred from diodes to thyristors, but also the aforementioned diode freewheeling effect can be eliminated, which makes it possible to extinguish the DC fault current [23].

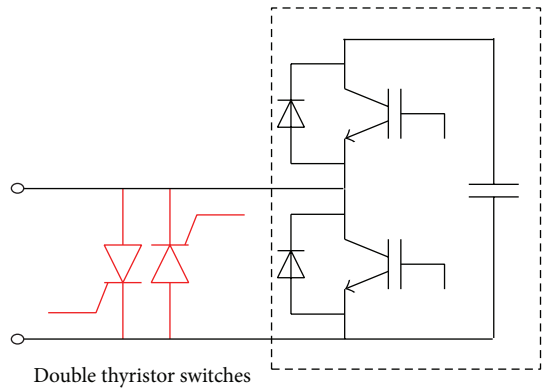


Figure 6: Double thyristor switches.

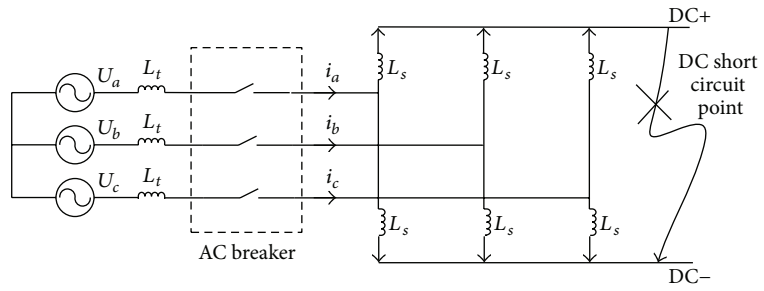


Figure 7: Equivalent circuit after adding protection under the overhead line fault.

In the proposed protection scheme, all IGBTs should be blocked as soon as DC fault is monitored. Simultaneously, all thyristors should be switched on to eliminate the rectifier mode of MMC. The fault equivalent circuit of MMC using the proposed protection scheme is shown in Figure 7. Different from the rectifier bridges, six MMC arms become six *R-L* branches after all thyristors are switched on. Because of the three-phase upper and lower arm symmetrical, DC line positive and negative electric potential is basically the same; DC side of MMC can be equivalent to withstand a relatively small voltage. DC short-circuit current gradually attenuates and disappears; the short point is naturally cut off. The role of the bypass switch is equivalent to convert DC fault into AC fault, thereby enabling the fault natural arcing.

*4.2. The Specific Protection Process as Shown in Figure 8.* Setting the protection action threshold of DC current is $I_{act}$ and the rated DC line current is $I_{dc}$ in normal operation mode. Generally, $I_{act}$ is set to be two or three times the size of $I_{dc}$. If $I_{dc} < I_{act}$, MMC converter works in the normal operation mode. If $I_{dc} > I_{act}$, it indicates that DC current increases because short circuit occurs in DC line and protection acts to make MMC converter work in fault protection mode.

Set the protection returning threshold of DC line current as $I_{ret}$ in fault protection mode. Generally, $I_{ret}$ is set to be a little bigger than zero. If $I_{dc} > I_{ret}$, it indicates that DC current was not completely interrupted and still makes MMC converter maintained in fault protection mode. If $I_{dc} < I_{ret}$, it indicates that short-circuit current has disappeared, so MMC converter goes into automatic recovery mode.

In automatic recovery mode, compare $I_{dc}$ with $I_{act}$ once again. If $I_{dc} < I_{act}$, it indicates that DC fault is nonpermanent fault, making MMC converter transfer to normal operation mode and restore power. If $I_{dc} > I_{act}$, it indicates that DC fault is permanent fault, so making protection act open the breaker of AC side and conduct outage maintenance.

When $t = 0.8$ s, bipolar short-circuit fault occurs in DC overhead lines and the simulation waveforms after adding protection are shown in Figures 9 and 10. System structure, fault point, and simulation parameters are shown in Figure 1, point 2 in Figure 1, and Table 1, respectively. Figure 9 shows the simulation waveform when nonpermanent fault occurs in overhead lines. Set $I_{act}$ as 3 kA and $I_{ret}$ as 0. After monitoring DC lines fault, fast blocking pulse acts to protect the switching devices in case of overcurrent and keeps the capacitor voltage of the submodule. The turning-on of bypass switch changes the structure of fault circuit and DC fault current attenuates. After the fault current arc extinguishing automatically, applied the zero level signal to bypass thyristors, until after 20 ms, all thyristors reliable shutdown, and then deblocking IGBT, MMC converter can achieve the automatic restart. Due to the fact that the fault is nonpermanent, the fault source has disappeared; the DC line will not cause the second-time DC line overcurrent and MMC converter works in the normal mode.

The simulation waveform of permanent fault is shown in Figure 10. Second-time overcurrent occurs when autorestart

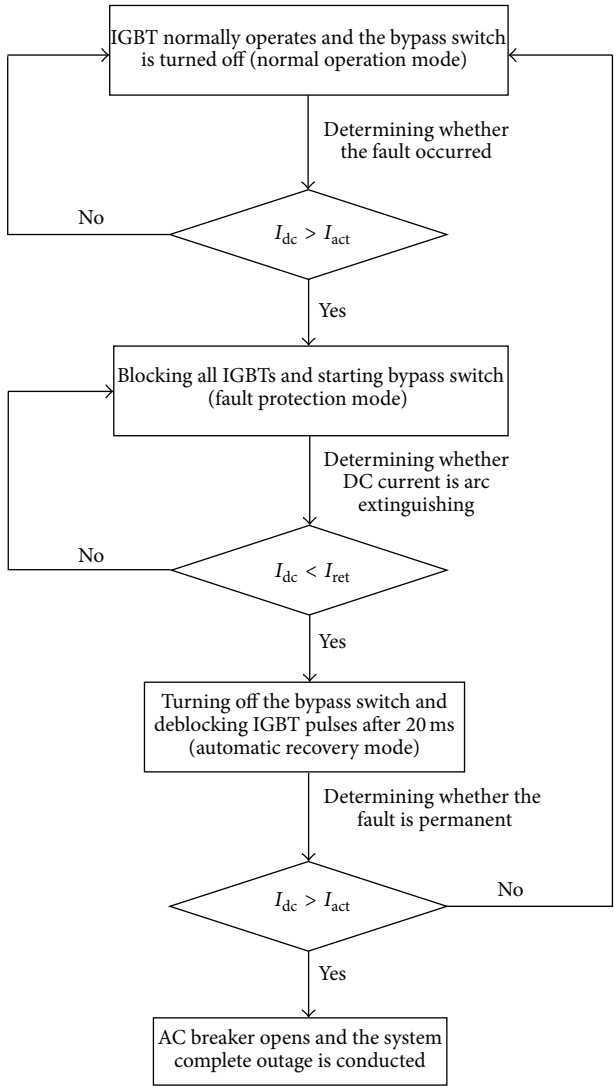


Figure 8: Specific flowchart of fault protection methods.

takes place. Protection AC breaker turns off, system stops totally, and it is time-consuming to recover power supply.

## 5. Fault Ride-through of Wind Farm Integration

When the wind farm connects AC grid through MMC-MTDC system, if AC grid of the receiving end fails, then the output power capacity of the receiving end will decrease, while power transmission of the wind farm will be not affected, so that active power transmission between the sending and receiving end becomes unbalanced and that will result in DC line voltage being too high. Therefore, control strategy must be taken to make MMC-MTDC system pass through AC grid fault of the receiving end, that is, the issue of fault ride-through (FRT). By installing unloading load in parallel in DC side to eliminate power imbalance in order to maintain a constant DC voltage. This paper further proposes the small and distributed unloading load which adopts a unified control, which can not only reduce the design and construction difficulty of the unloading load, but also can improve the reliability of the unloading load.

The unloading load can be installed in parallel in DC side which is a resistor controlled by IGBT, as shown in Figure 11. When triggering IGBT to conduct, the unloading load begins to consume energy; if IGBT works in PWM mode, the energy consumption of the unloading load can be quantitatively controlled. The unloading load can consume power difference that MMC-MTDC system cannot eliminate so as to maintain DC line voltage constant. The control strategies of suppressing DC over voltage are as follows:

(1) Monitoring DC line voltage to determine whether DC line is overvoltage.

(2) Setting overvoltage allowable value that is typically 1.01 to 1.05 times of rated voltage.

(3) When the monitored value of DC voltage rises more than the allowable value, measuring the input and

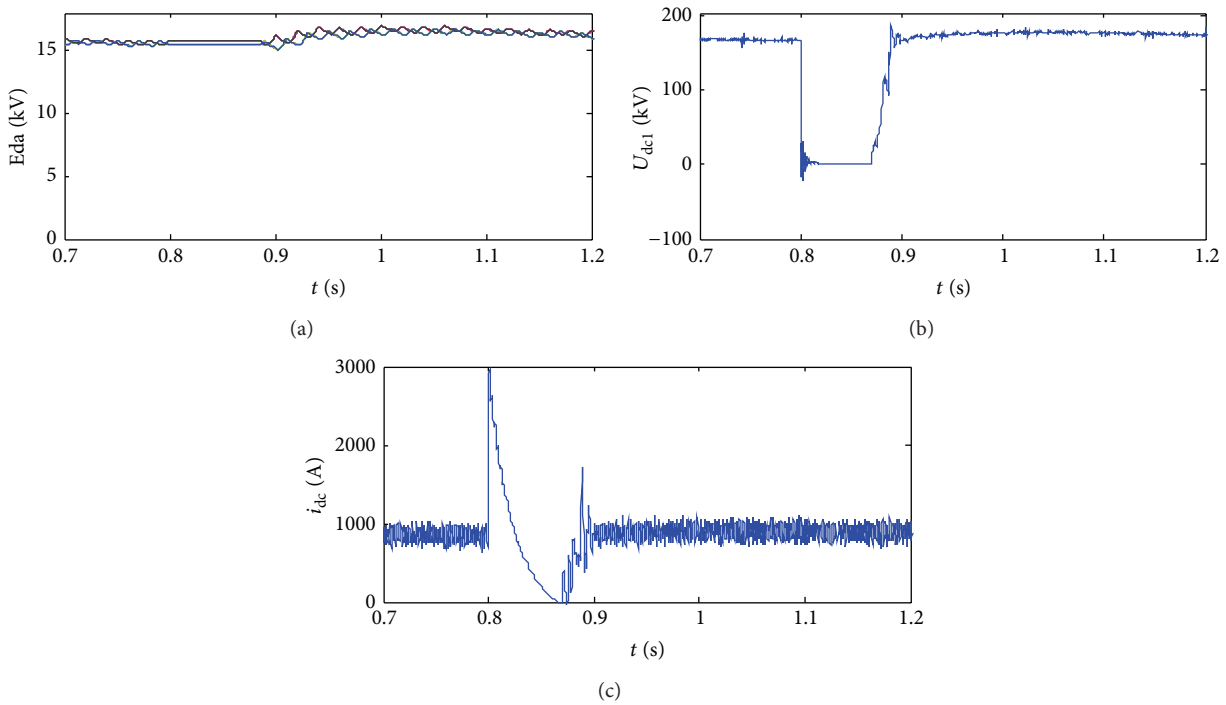


Figure 9: Simulation waveforms in nonpermanent fault after adding protection. (a) Submodule capacitor voltage of phase *a*. (b) DC line voltage. (c) DC line current.

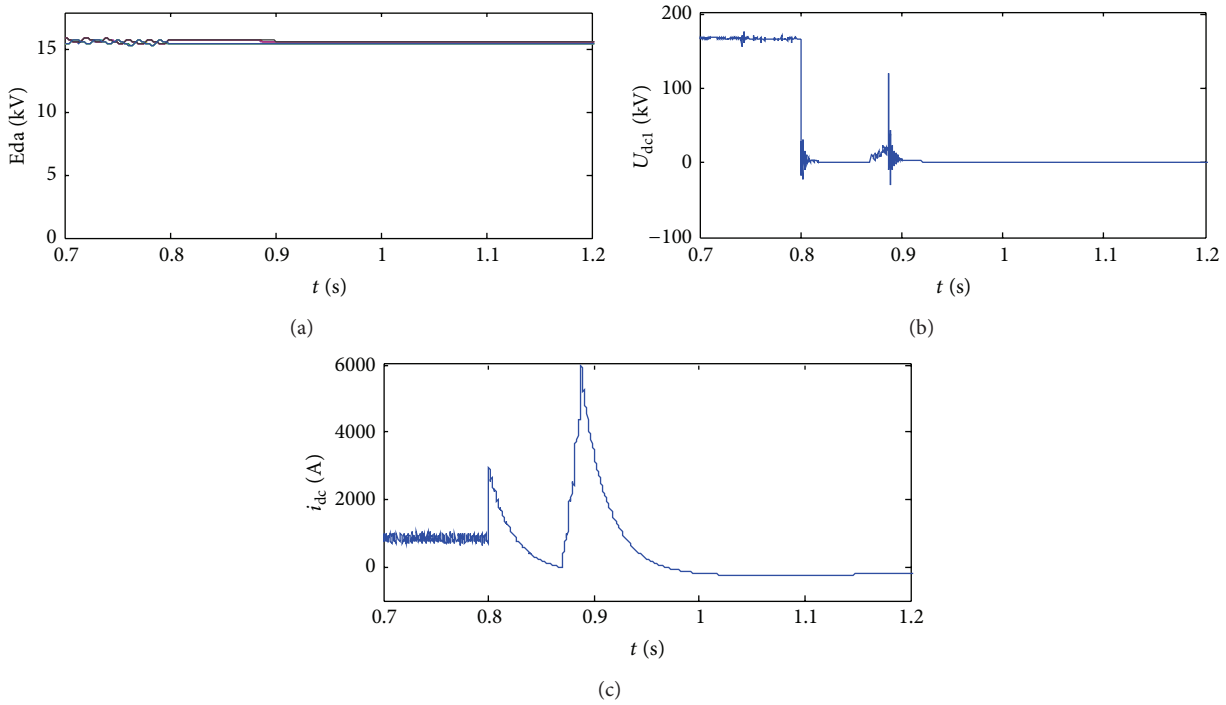


Figure 10: Simulation waveforms in permanent fault after adding protection. (a) Submodule capacitor voltage of phase *a*. (b) DC line voltage. (c) DC line current.

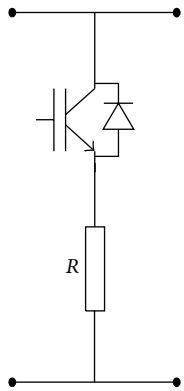


Figure 11: Structure of the unloading load.

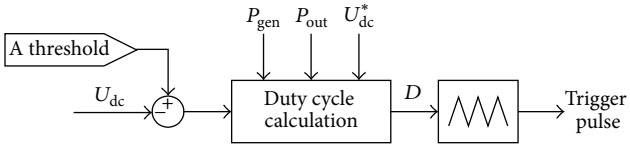


Figure 12: Control block diagram of the unloading load.

output power of transmission system $P_{gen}$, $P_{out}$. In order to eliminate the second harmonic fluctuations brought by negative sequence component, $P_{gen}$ and $P_{out}$ need to filter by low pass filter (LPF).

The duty cycle of IGBT can be calculated according to power difference, as in the following formula; the control block diagram is shown in Figure 12:

$$D = \frac{\sqrt{\left(P_{gen} - P_{out}\right) \cdot R}}{U^*_{dc}}. \quad (3)$$

This paper puts forward small and distributed unloading load by a unified control. That is,

(1) Installed locations dispersion: it should be set at DC outlet of MMC2 and MMC3 in the wind farm side rather than only at DC outlet of MMC1.

(2) Installed capacity dispersion: multiple smaller capacity unloading load should be chosen, whose capacity is proportional to the capacity of MMC converter station in the wind farm side, respectively, rather than only a large unloading load matching with MMC1. This not only reduces the design and construction difficulty of the unloading load but also improves the reliability of the unloading load.

(3) Unified control by using a set of controller: set the input power as $P_{gen\_i}$ $(i = 1, 2, \ldots, n)$ and the output power as $P_{out}$. According to the proportion of rated capacity $P_{N\_i}$ to allocate the balance of power, and respectively calculate the turn-on duty cycle of IGBT of each unloading load $D_i$ $(i = 1, 2, \ldots, n)$, as in the following formula; the control block diagram is shown in Figure 13:

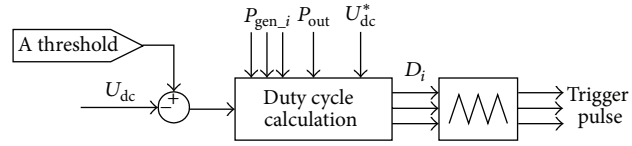


Figure 13: New control block diagram of the unloading load.

Table 2: Simulation parameters of three-terminal MMC-HVDC system.

| Parameters | Value |
|---|---|
| Rated capacity of AC grid | 300 MVA |
| Rated capacity of wind farm 1 | 100 MVA |
| Rated capacity of wind farm 2 | 200 MVA |
| Transformer ratio of MMC1 ($Y/\Delta$) | 220 kV/150 kV |
| Transformer ratio of MMC1 ($Y/\Delta$) | 110 kV/150 kV |
| Transformer ratio of MMC1 ($Y/\Delta$) | 110 kV/150 kV |
| Voltage of DC bus | ±150 kV |
| Number of submodules of bridge arm | 4 |
| Control mode of MMC1 | $U_{dc}, Q$ |
| Control mode of MMC2 | $V, f$ |
| Control mode of MMC3 | $V, f$ |
| Modulation strategy | Carrier phase-shifted modulation |
| Capacitor voltage balancing strategy | Capacitor voltage sort |

$$D_i = \frac{\sqrt{\left(\sum_{i=1}^{n} P_{gen\_i} - P_{out}\right) \cdot \left(P_{N\_i} / \sum_{i=1}^{n} P_{N\_i}\right) \cdot R_i}}{U^*_{dc}}. \quad (4)$$

Taking grounding short-circuit fault of phase $a$, for example, which corresponds to point 1 in Figure 14, the simulation parameters are shown in Table 2. The simulation waveforms according to the above control strategy are shown in Figure 15. The out power of wind farm 1 is 160 MW/10 Mvar and the out power of wind farm 2 is 80 MW/20 Mvar in steady-state operation. Unloading load 1 is placed in MMC2 and the resistance value is 900 ohm; the maximum 100 MW power can be consumed by unloading load 1. Unloading load 2 is placed in MMC3 and the resistance value is 1800 ohm; the maximum 50 MW power can be consumed by unloading load 2. The trigger threshold of both unloading loads is set to 1.05 times of DC voltage reference value. When $t = 1.5$ s, the grounding short-circuit fault of phase $a$ occurs, the asymmetric component of AC line voltage emerges (Figure 15(a)). Due to the short-circuit fault, the active power transmission of MMC1 drops to about 120 MW (Figure 15(b)). But due to the inertia effect, active power transmission sent by two wind farms remains 160 MW and 80 MW (Figure 15(c)). The imbalance of active power transmission is reflected to DC voltage and then the unloading load is triggered to consume excess energy, so that making DC voltage in the vicinity of

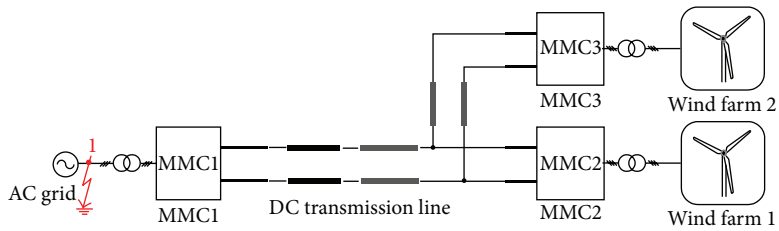


Figure 14: Structure of three-terminal MMC-HVDC system.

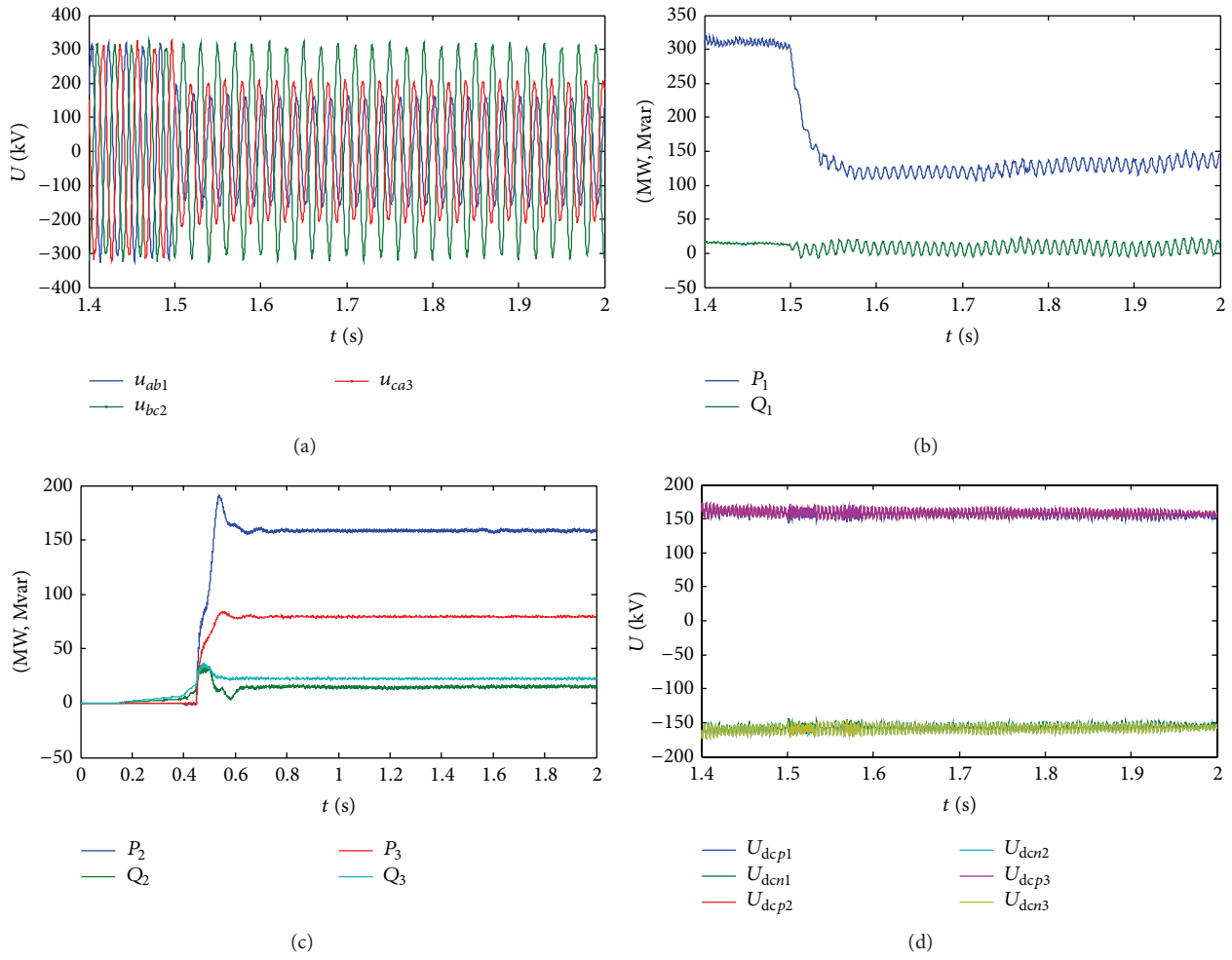


Figure 15: Simulation waveforms of grounding short-circuit fault of phase *a* in AC grid. (a) Line voltage of AC grid. (b) Power transmission of MMC1. (c) Power transmission of MMC2 and MMC3. (d) DC bus voltage.

the reference value (Figure 15(d)) and ensuring that MMC-MTDC system maintains the maximum power transmission during fault.

## 6. Conclusions

This paper firstly described submodule fault characteristics and proposed submodule redundancy protection for MMC-MTDC system. Secondly, we proposed a protection scheme to implement fast fault clearance and automatic recovery for nonpermanent faults on DC lines. Lastly, a new fault ride-through method for wind farm connection was proposed. Our future work would focus on the experiment using RT-LAB.

## Conflict of Interests

The authors declare no conflict of interests.

## Acknowledgment

This work was supported by the Fundamental Research Funds for the Central Universities (2015YJS162).

## References


[1] X. Hu, N. Murgovski, L. M. Johannesson, and B. Egardt, "Comparison of three electrochemical energy buffers applied to a hybrid bus powertrain with simultaneous optimal sizing and energy management," *IEEE Transactions on Intelligent Transportation Systems*, vol. 15, no. 3, pp. 1193–1205, 2014.

[2] X. Hu, N. Murgovski, L. M. Johannesson, and B. Egardt, "Optimal dimensioning and power management of a fuel cell/battery hybrid bus via convex programming," *IEEE/ASME Transactions on Mechatronics*, vol. 20, no. 1, pp. 457–468, 2015.

[3] C. Sun, S. J. Moura, X. Hu, J. K. Hedrick, and F. Sun, "Dynamic traffic feedback data enabled energy management in plug-in hybrid electric vehicles," *IEEE Transactions on Control Systems Technology*, vol. 23, no. 3, pp. 1075–1086, 2015.

[4] S. Chu and A. Majumdar, "Opportunities and challenges for a sustainable energy future," *Nature*, vol. 488, no. 7411, pp. 294–303, 2012.

[5] D. MacKay, *Sustainable Energy: Without the Hot Air*, UIT Cambridge, Cambridge, UK, 2009.

[6] R. Marquardt, "Stromrichterschaltungen mit Verteilten Energiespeichern," German Patent DE10103031A1, 2001.

[7] S. Allebrod, R. Hamerski, and R. Marquardt, "New transformerless, scalable modular multilevel converters for HVDC-transmission," in *Proceedings of the IEEE Power Electronics Specialists Conference (PESC '08)*, pp. 174–179, IEEE, Rhodes, Greece, June 2008.

[8] J. Peralta, H. Saad, S. Dennetière, J. Mahseredjian, and S. Nguefeu, "Detailed and averaged models for a 401-level MMC-HVDC system," *IEEE Transactions on Power Delivery*, vol. 27, no. 3, pp. 1501–1508, 2012.

[9] S. Xu, H. Rao, Q. Song, W. Liu, and X. Zhao, "Experimental research of MMC based VSC-HVDC system for wind farm integration," in *Proceedings of the IEEE 22nd International Symposium on Industrial Electronics (ISIE' 13)*, pp. 1–5, May 2013.

[10] G. Ramtharan, A. Arulampalam, J. B. Ekanayake, F. M. Hughes, and N. Jenkins, "Fault ride through of fully rated converter wind turbines with AC and DC transmission systems," *IET Renewable Power Generation*, vol. 3, no. 4, pp. 426–438, 2009.

[11] H. G. Jeong, U. M. Choi, and K. B. Lee, "Control strategies for wind power systems to meet grid code requirements," in *Proceedings of the 37th Annual Conference on IEEE Industrial Electronics Society (IECON '11)*, pp. 1250–1255, IEEE, Melbourne, Australia, November 2011.

[12] C. Feltes, H. Wrede, F. W. Koch, and I. Erlich, "Enhanced fault ride-through method for wind farms connected to the grid through VSC-based HVDC transmission," *IEEE Transactions on Power Systems*, vol. 24, no. 3, pp. 1537–1546, 2009.

[13] S. K. Chaudhary, R. Teodorescu, P. Rodriguez, and P. C. Kjar, "Chopper controlled resistors in VSC-HVDC transmission for WPP with full-scale converters," in *Proceedings of the 1st IEEE-PES/IAS Conference on Sustainable Alternative Energy (SAE '09)*, pp. 1–8, IEEE, Valencia, Spain, September 2009.

[14] S. Liu, Z. Xu, W. Hua, G. Tang, and Y. Xue, "Electromechanical transient modeling of modular multilevel converter based multi-terminal hvdc systems," *IEEE Transactions on Power Systems*, vol. 29, no. 1, pp. 72–83, 2014.

[15] G. Zhang, Z. Xu, and H. Liu, "Supply passive networks with VSC-HVDC," in *Proceedings of the IEEE Power Engineering Society Summer Meeting*, vol. 1, pp. 332–336, July 2001.

[16] G. Tang, *HVDC Based on Voltage Source Converter*, China Electric Power Press, Beijing, China, 2010.

[17] G. Tang, X. Luo, and X. Wei, "Multi-terminal HVDC and DC-grid technology," *Proceedings of the Chinese Society of Electrical Engineering*, vol. 33, no. 10, pp. 8–17, 2013.

[18] X. Zhang, C. Zhao, H. Pang, and C. Lin, "A control and protection scheme of multi-terminal DC transmission system based on MMC for DC line fault," *Automation of Electric Power Systems*, vol. 37, no. 15, pp. 140–145, 2013 (Chinese).

[19] J. Xu, C. Zhao, and B. Zhang, "Control design and operational characteristics comparation for VSC-HVDC supplying active/passive networks," in *Proceedings of the 6th IEEE Conference on Industrial Electronics and Applications (ICIEA '11)*, pp. 1381–1386, June 2011.

[20] P. Hu, D. Jiang, Y. Zhou, Y. Liang, J. Guo, and Z. Lin, "Energy-balancing control strategy for modular multilevel converters under submodule fault conditions," *IEEE Transactions on Power Electronics*, vol. 29, no. 9, pp. 5021–5030, 2014.

[21] M. Guan and Z. Xu, "Redundancy protection for sub-model faults in modular multilevel converter," *Automation of Electric Power Systems*, vol. 35, no. 16, pp. 94–104, 2011 (Chinese).

[22] W. Song and A. Q. Huang, "Fault-tolerant design and control strategy for cascaded H-bridge multilevel converter-based STATCOM," *IEEE Transactions on Industrial Electronics*, vol. 57, no. 8, pp. 2700–2708, 2010.

[23] X. Li, Q. Song, W. Liu, H. Rao, S. Xu, and L. Li, "Protection of nonpermanent faults on DC overhead lines in MMC-based HVDC systems," *IEEE Transactions on Power Delivery*, vol. 28, no. 1, pp. 483–490, 2013.